Morphological Effects on the Bulk Polymerization of Trioxane in the Solid State by γ-Radiation

GABOR KISS,* KLARA KISS,† A. J. KOVACS, and J. C. WITTMANN,
Centre de Recherches sur les Macromolécules (C.N.R.S. et U.L.P.), 6, Rue Boussingault, 67 083 Strasbourg, France

Synopsis

The solid-state polymerization by γ-radiation and postpolymerization of bulk samples of trioxane has been investigated. Different thermal treatment results in radically different initial morphologies of the melt-crystallized trioxane which in turn have a profound influence on the yield and morphology of the resulting poly(oxymethylene) (POM). The polymerization yield increases in the following series: melt-crystallized trioxane with an "opaque" (small grains) morphology, as-grown needles, trioxane with a "quasi-transparent" morphology, and finally thermally oriented crystals. Furthermore, little additional POM is formed during repeated polymerization cycles. The observation of an extensive nodulation of the polymer fibrils when the yield is high is consistent with a multiple-stage growth model for the solid-state polymerization of trioxane.

INTRODUCTION

The polymerization of crystalline trioxane (TOX) to crystalline poly(oxymethylene) (POM) is a process which can be expected to occur quite easily, since the C—O bonds broken to open the TOX rings are immediately reformed upon reaction to form the polymer; and as relief of ring strain is not significant either, the change in bond energies is approximately zero. The observed heat of polymerization of 1.88 kcal/mol TOX must therefore be due to a difference in lattice energies between the crystalline TOX and the crystalline POM.[1] Furthermore, since little change in entropy would be expected in transforming crystalline monomer to crystalline polymer, it follows that the TOX is thermodynamically unstable with respect to the POM.[1] Thus, if monomer morphology is favorable, the monomer will convert to polymer, given a perturbation sufficiently energetic to overcome the potential barrier involved in opening the TOX rings.

It is not surprising therefore that TOX can be provoked into polymerizing by a wide variety of stimuli. Spontaneous polymerization during sublimation of the crystals was reported as early as 1922.[2] More recently, van der Heidje reported that any phase change involving the crystalline monomer can trigger polymerization.[3] Polymerization of TOX in the solid state has also been induced by a variety of forms of high-energy radiation, e.g., γ-ray,[4,5] x-ray,[6,7] electron beams,[8] and α-particles.[9] A variety of chemical initiators has also been shown to be effective,[10,11] and even shock waves can provoke this reaction.[12]

Since the solid-state polymerization of TOX can be accomplished in so many ways, any given set of experimental conditions might involve a variety of pathways, or even several pathways simultaneously. As a consequence, it appears

* Present address: Celanese Research Co., 86 Morris Ave., Summit, NJ 07901, U.S.A.
† Address: Stauffer Chemical Co., Livingston Ave., Dobbs Ferry, NY 10522, U.S.A.

Journal of Applied Polymer Science, Vol. 26, 2485–2500 (1981)
 CCC 0021-8995/81/072485-15$01.60

that the solid-state polymerization of TOX could well be too complex or ill-defined a phenomenon to speak of a single "reaction mechanism" outside of the context of particular experimental conditions. (These comments naturally apply to the work reported herein, and the reader should be cognizant of this when considering the results.) In fact, many conflicting observations have been reported in the literature on this phenomenon.

A variety of values for the activation energy ranging from 0 to 68.5 kcal/mol have been reported.[13-18] The reaction is generally considered to proceed via a cationic mechanism, but opinions differ as to the nature of the active species.[19-22] There is disagreement as to the effect of oxygen on the kinetics and yield of the reaction[14,16,23,24] and as to whether there is an induction period.[6-8,25-27] Some experiments have shown that the active species formed by irradiation is extremely stable,[28-30] but this point is contested in another work.[27]

Another intriguing paradox is the degree of control exerted by the monomer lattice on the reaction. The resulting polymer is almost 100% crystalline[5] and extremely highly ordered (several early investigators reported that single crystals of TOX give rise to single crystals of POM with no apparent change in shape or size,[31,32]) and it has been observed that the twin structure which occurs is well defined,[5] leading to the widespread use of the term "topochemical" to describe this reaction. That is, polymerization was thought to occur without requiring monomer molecules to leave their lattice positions. On the other hand, it was observed that the maximum polymerization rate is reached at a temperature just below the melting temperature of TOX,[33,34] implying that extensive molecular mobility is required. Also the mismatch between the TOX and the POM unit cells leads to axial dilation and lateral contraction during polymerization,[6] casting further doubt on a strict topochemical reaction. A solid–gas–solid mechanism has been proposed in which TOX sublimates and then adds to the growing polymer from the vapor phase.[22] Most workers have reported that polymer chain growth stops at grain boundaries, but at least one has observed growth to continue into adjacent TOX grains without change in direction.[35] The possible role of dislocation lines in determining the direction of chain growth, rather than the monomer lattice, has also been considered.[36]

The structure of the resulting polymer fibrils is at present less controversial. Dark-field electron microscopy has established that each fibril contains sections exhibiting the so-called Z-orientation (main crystal, parallel to the threefold axis of the parent TOX crystal) and W-orientation (twinned subcrystal[5] at an angle of 76.7°) distributed randomly along the fibril.[6,9,37] The average length of *Z* and *W* crystallites has been reported as 550 and 250 Å, respectively,[38] and a model of randomly kinked bundles of polymer chains has been proposed.[9] This implies that the POM crystals are not composed of extended chain polymer, as originally thought.[39,40]

Our interest in the solid-state polymerization of TOX stems not from a desire to resolve some of the conflicts in the literature mentioned above, but is a by-product of work performed in this laboratory on the production of "*in situ* composites" of POM/polycaprolactone (PCL) and POM/poly(ethylene oxide) (PEO) by "*in situ* solid-state polymerization" of TOX crystals grown within hypoeutectic (TOX-rich) mixtures of TOX/PCL and TOX/PEO. Early failures to produce POM in such mixtures forced us to backtrack to trying to produce

POM from pure TOX under the conditions imposed by the "*in situ* polymerization" technique. As a result, most of the work reported below involves bulk samples rather than single crystals or thin films used in most previous investigations. This led us to observe the phenomena described below which probably did not occur under the experimental conditions used by previous investigators.

All the results presented below lead inescapably to the conclusion that the morphology of the parent TOX crystals plays a crucial role in the yield of the reaction, an observation difficult to reconcile with any model which involves a sublimation step. Our results also show once again the unexpectedly important role played by experimental conditions and that unidentified, and therefore uncontrollable, factors are involved.

EXPERIMENTAL

As has often been pointed out, a crucial factor in the solid-state polymerization of TOX is the purity, particularly the dryness, of the monomer. The purification system used to prepare gram quantities of purified TOX is illustrated in Figure 1. Several grams of commercial TOX (Merck) and freshly crushed calcium hydride were introduced into flask 1 and heated to approximately 90°C to melt the TOX crystals. The flask was swirled for several minutes to maximize the contact between CaH_2 and molten TOX. After cooling to room temperature, the flask was installed in the apparatus as shown and a vacuum pulled to a level of approximately 20 torr. A flow of ultradry nitrogen was then started, and with the capillary restricting the nitrogen flow, the vacuum was stabilized at 80–100

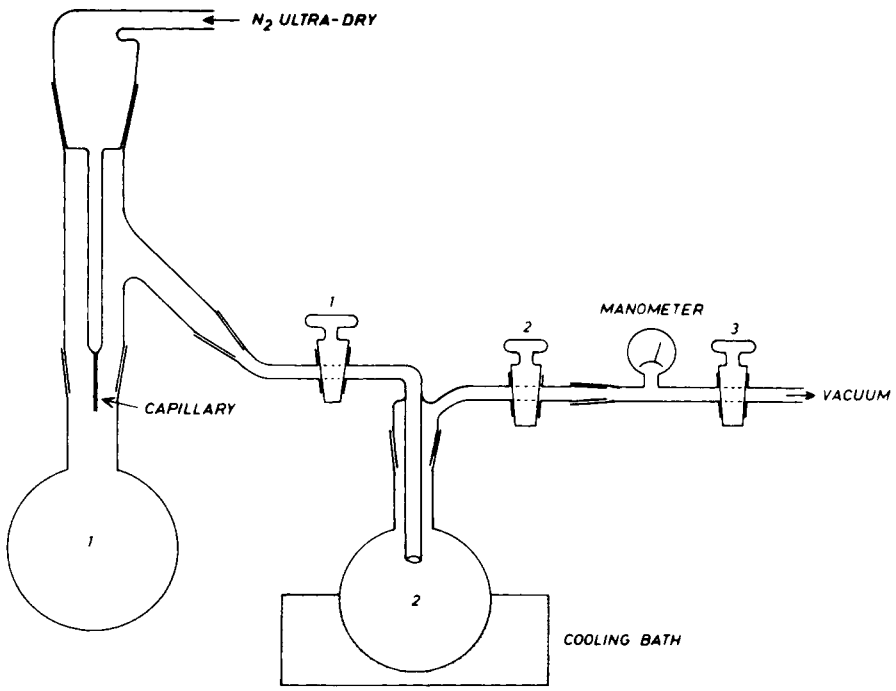

Fig. 1. Schematic diagram of trioxane purification apparatus.

torr. A dry ice/isopropanol slush was used as a cooling bath and the receptacle flask 2 immersed halfway. Since TOX sublimates rapidly at room temperature, TOX vapor is always present in flask 1. The vapor is entrained by the nitrogen flow and condenses in flask 2. When the process is started, very long, very thin needles fill the lower half of flask 2 almost immediately. These needles thicken with time and eventually become covered with a coarse overgrowth. It is very important to avoid any leaks: even though the vacuum in the system is not high, if any leak exists atmospheric moisture will be sucked in and deposited on the growing TOX needles. With this system several grams of pure TOX were obtained in 2–3 h, after which stopcock 3 was closed and nitrogen allowed to fill the system. After reheating to room temperature, flask 2 was removed and the TOX needles transferred quickly to 5-mm-i.d. sample tubes. We recognize that some atmospheric moisture may have been absorbed during the short time that the TOX was exposed to air (and that even such short exposure can be significant for very moisture sensitive materials[41]), but short of performing all operations in a dry glove box, this was unavoidable.

Various initial morphologies of the parent TOX were obtained by (1) no action, so that the sample consisted of trioxane needles; (2) melting and recrystallization to form bulk samples (more details given in results section); and (3) melting, recrystallization, and subsequent one-pass thermal orientation through a gradient of 9.2°C/mm using the temperature gradient oven shown in Figure 2.

The irradiation of the samples was performed in a ^{60}Co γ-ray source at an ambient temperature of about 30°C. An exposure of 5 h gave a dose of 5×10^5 rad as measured by Fricke dosimetry. Postpolymerization was achieved at 50°C for 12 h.

Conversions were determined by weighing polymerized samples before and after sublimation of residual trioxane. Three separate measurements were made on different pieces of each sample.

RESULTS AND DISCUSSION

Thermal History of Bulk Samples

We observed that the thermal treatment of trioxane needles molten to produce bulk samples had a profound effect on both the initial morphology of the parent TOX sample and the degree of conversion to polymer. (Of course, the differences in monomer morphology translated directly to differences in morphology of the resultant polymer.)

When purified TOX needles were heated to 70°C until complete fusion took place (typically 1–2 min) and then rapidly cooled to room temperature, the bulk sample crystallized to a quasi-transparent mass consisting of large crystals with domain boundaries which were visible with the naked eye. A macrophotograph [Fig. 3(a)] taken with reflected light on a black background shows that this sample is almost transparent, except for featherlike white features which are reflections from central voids created by shrinkage of the sample during crystallization. On the other hand, if retained in the molten state for times on the order of 15 min or longer, the bulk sample crystallizes to a fairly opaque mass. The macrophotograph in Figure 3(b) shows the dull, diffuse reflection from the many tiny crystal grains making up this sample.

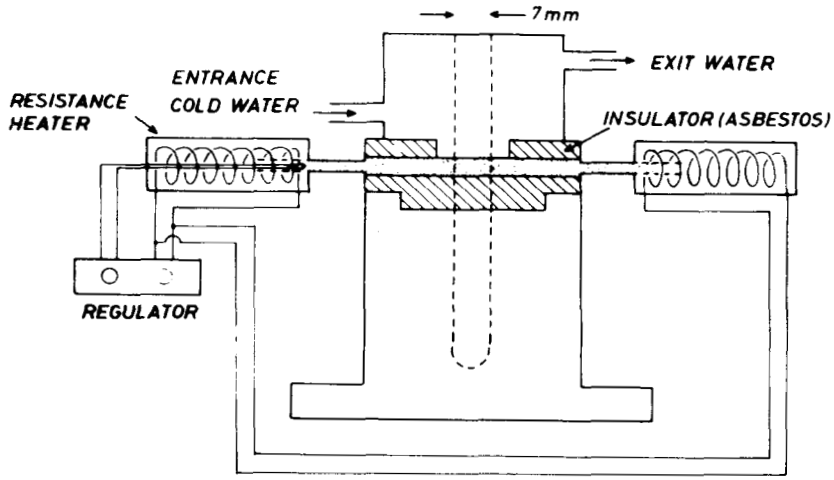

Fig. 2. Schematic diagram of thermal gradient oven.

Similar samples after irradiation and postpolymerization are shown in Figure 4. The difference in size of the resulting POM crystals is obvious and reflects the difference in size of the parent TOX crystals. The degree of conversion of the two types of initial morphologies was also very different. A total of 37 different samples exhibiting the quasi-transparent initial morphology gave an average yield of 37.1% with a standard deviation of 10.25. As shown by the large

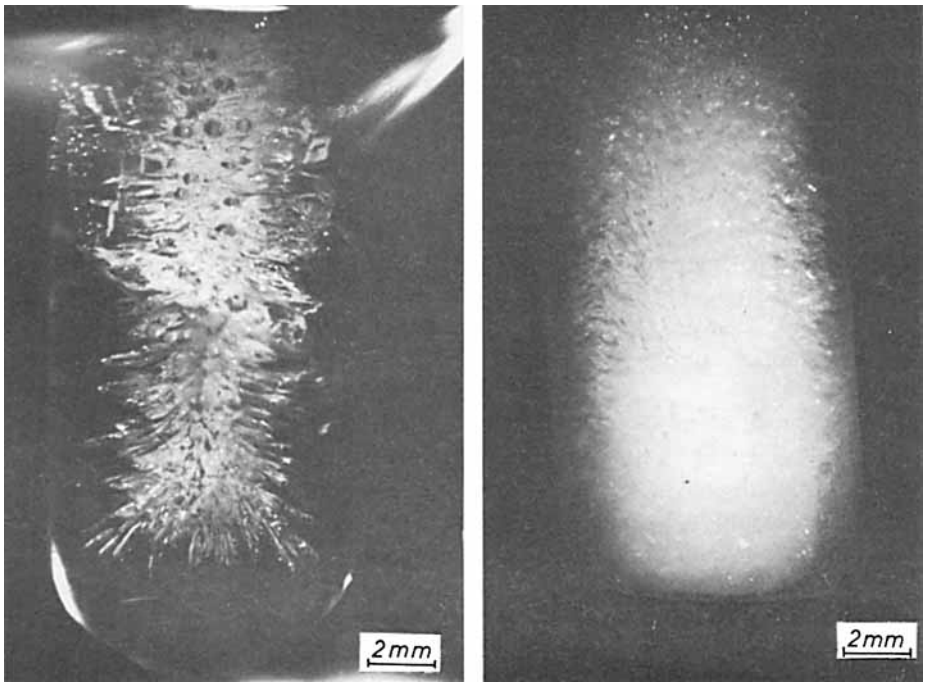

(a) (b)

Fig. 3. (a) Bulk trioxane in quasi-transparent morphology. (b) Bulk trioxane in opaque morphology.

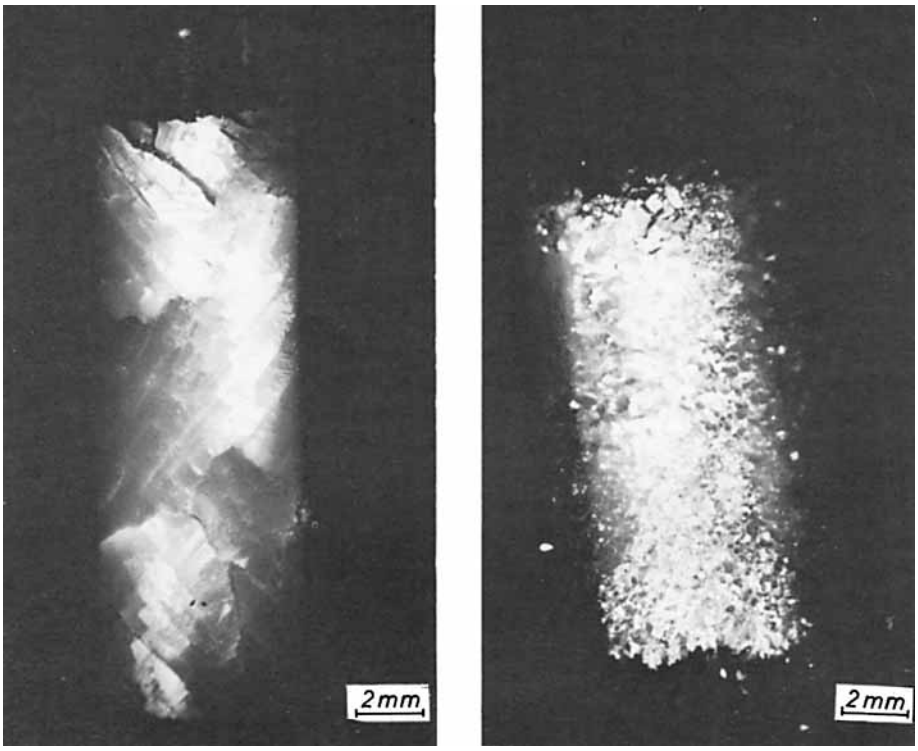

(a) (b)

Fig. 4. (a) Poly(oxymethylene) from solid-state polymerization of bulk trioxane in quasi-transparent morphology. (b) Poly(oxymethylene) from solid-state polymerization of bulk trioxane in opaque morphology.

standard deviation, the yields were widely scattered, with extremes of 11.5 and 57.8% for individual measurements. Three measurements were made on each sample, and variations of up to 20 percentage points were observed within samples, indicating poor homogeneity. On the other hand, the conversions of the initial opaque morphology were much lower and depended very much on the time and temperature that the TOX was kept molten.

A series of five samples maintained at 70°C for various times gave the following yields:
1–2 min (quasi-transparent), 38.3 ± 5.1; 5 min (opaque), 17.2 ± 8.7; 15 min (opaque), 6.7 ± 6.6; 1 h (opaque), 1.2 ± 2.5. Again the large standard deviation reveals a high degree of scatter both between samples and within samples. For an extreme example, two pieces of the same sample maintained molten at 70°C for 15 min gave yields of 11.7 and 0%. Storage at 90°C for ½ h reduced the yield to practically zero in all cases.

Further experiments revealed that the effect of maintaining the TOX molten for long times could be reversed by quenching the tip of the sample tube in dry ice/isopropanol or by isothermal crystallization at 50°C, as manifested both by the morphology and the yield. This series of experiments is summarized in Table I. Note that the yield after 1 h at 70°C is atypically high for this particular sample (cf. the series of experiments at 70°C referred to above).

TABLE I

Time in molten state at 70°C	Crystallization conditions	Appearance of sample	Polymer yield (individual measurements on same sample), %
Approximately 1–2 min	quench to room temperature (25°C)	quasi-transparent	45.3, 42.3, 43.5
Approximately 1–2 min	quench to −78°C	quasi-transparent	48.1, 46.8, 48.1
Approximately 1–2 min	quench tip to −78°C, remainder at higher temp.	opaque at tip, quasi-transparent elsewhere	35.5, 31.5, 29.6 (in quasi-transparent portion)
Approximately 1–2 min	crystallization at 50°C	quasi-transparent	31.4, 44.2, 44.7
One hour	quench to 25°C	opaque	18.7, 11.3, 17.9
One hour	quench to −78°C	opaque	6.4, approx. 0, approx. 0
One hour	quench tip to −78°C remainder at higher T	opaque at tip, quasi-transparent elsewhere	36.4, 36.3, 39.2 (in quasi-transparent portion)
One hour	crystallization at 50°C	quasi-transparent	38.4, 26.6, 37.9

Figures 5 and 6(a) show SEM micrographs of a large POM crystal obtained from TOX in the quasi-transparent morphology and a cluster of small POM grains obtained from TOX in the opaque morphology. Some of these grains show large voids which are not seen in the large crystals. A more detailed view is shown in Figure 6(b). These voids appear to be spaces left by trapped air bubbles. Significantly, the voids are nearly cylindrical, with their axes parallel to the polymer fibrils and hence the growth direction of the parent TOX crystals. This

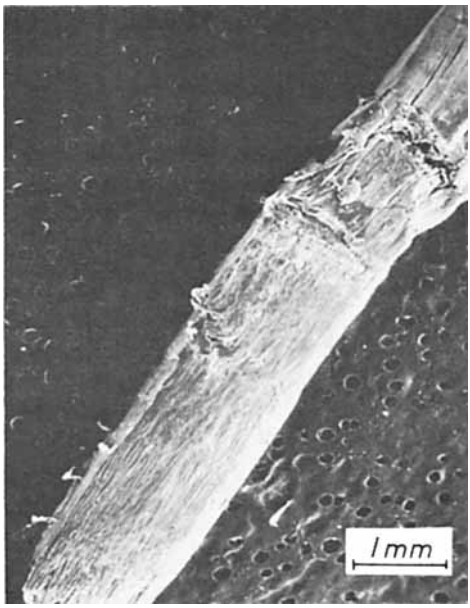

Fig. 5. Poly(oxymethylene) domain from solid-state polymerization of bulk trioxane in quasi-transparent morphology.

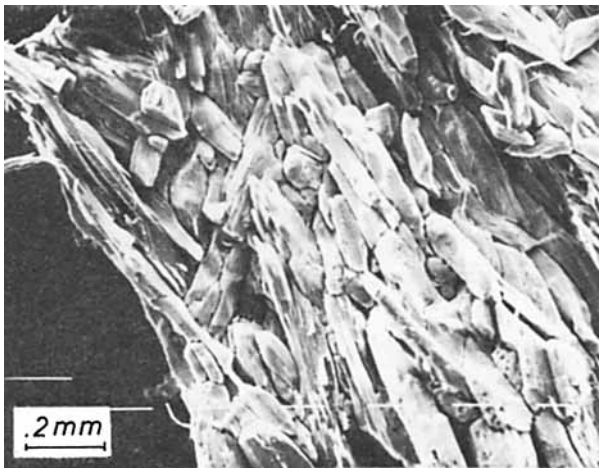

(a)

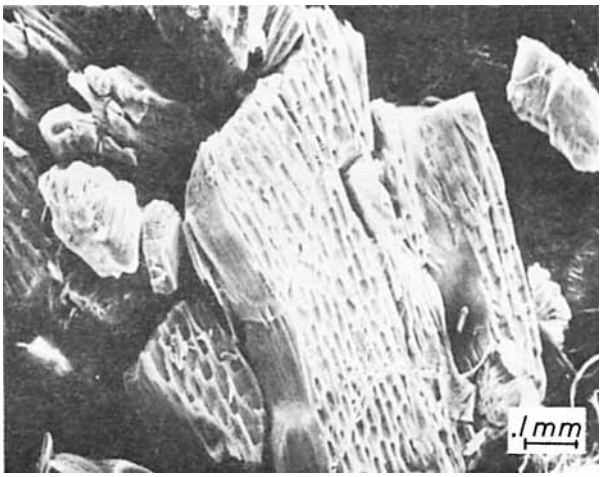

(b)

Fig. 6. (a) Cluster of poly(oxymethylene) grains from solid-state polymerization of bulk trioxane in opaque morphology. (b) Single grains showing cylindrical voids.

is what would be expected of spherical air bubbles trapped in a unidirectionally growing crystal.

One of the questions one must ask is, why do these different thermal treatments produce such radically different initial morphologies? It seems quite clear that in order to produce large numbers of small grains, a much higher density of nuclei must have been generated at a given stage of the thermal treatment. The possible presence of foreign bodies would not explain the effects of thermal history. It is also unlikely that residual nuclei could persist in the molten TOX for periods on the order of minutes. Furthermore, even so, the effect would be the opposite from that observed, i.e., longer residence times in the melt would reduce the concentration of residual nuclei rather than increase it. The possibility of some kind of degradation effect can also be dismissed, as the thermal treatment was very mild and TOX is known to be thermally stable to much higher

temperatures.[42] Also the latter two hypotheses can be rejected in view of the "reversibility" of the phenomenon as described above and summarized in Table I.

The observed effect of thermal history may be tentatively attributed to the dissolution of increased quantities of air with time in the molten state. TOX needles of course contain no air, and so they melt to a liquid which contains little dissolved air. Holding the melt for longer times allows increasing quantities of air from inside the sample tube to dissolve in the molten trioxane.

Once a crystal of TOX starts to grow from a supercooled melt containing a substantial amount of dissolved air, since the air cannot be incorporated into the lattice, it is expelled in the form of bubbles some of which are trapped in the growing crystal. It is well known that nucleation is greatly enhanced by mechanical actions such as agitation and/or turbulence. The disturbance of the surrounding supercooled melt by air bubbles could well result in an increased number of nuclei, thereby reducing the size of the crystals formed. Such an explanation is further substantiated by the fact that crystallization was rather slow but continuous when forming the quasi-transparent morphology, whereas the opaque morphology forms rather abruptly throughout the sample tube. The observation that the effect of maintaining TOX molten for extended periods of time could be erased by adequate thermal treatments can also be rationalized on the basis of this hypothesis. Crystallization at 50°C occurs at a much slower rate than at room temperature, so that air bubbles can easily float away without being trapped. Furthermore, the disturbance of the surrounding melt by the evolution of air bubbles would be less effective in the creation of nuclei than in a melt which is supercooled to a much greater extent. Similarly, quenching the tip of the sample tube to −78°C causes crystallization to start at the bottom and proceed upward while the remainder of the melt is still at a higher temperature. Therefore, the crystallization is again relatively slow, giving air bubbles a chance to float away rather than being trapped in the advancing crystal.

Finally, the diffuse, milky appearance of the sample is also what one would expect from a large number of tiny inclusions, such as air bubbles, in the TOX crystals.

Thermally Oriented Samples

The trioxane passed through the temperature gradient oven shown in Figure 2 emerged visibly more transparent; the central voids due to contraction during crystallization were smaller and boundaries between crystals were hardly visible. The TOX crystals were highly oriented along the tube axis and presumed to extend along the entire length of the sample tube. Figure 7 shows POM crystals from TOX oriented within thin capillaries (i.d. $\sim$ 1 mm). The polymer crystals again retained the morphology of the parent TOX crystals. Material which was not passed through the melting zone polymerized into POM grains of various sizes (upper portions of Fig. 7). The material which did pass through the melting zone produced indefinitely long POM crystals parallel to the capillary axis (lower portions of Fig. 7).

Bulk samples pulled through the temperature gradient at 0.785 and 6.6 mm/min gave yields of 44.5 ± 6.6 and 51.0 ± 6.5%, respectively. It thus seems that the additional crystal perfection imparted by the thermal orientation in-

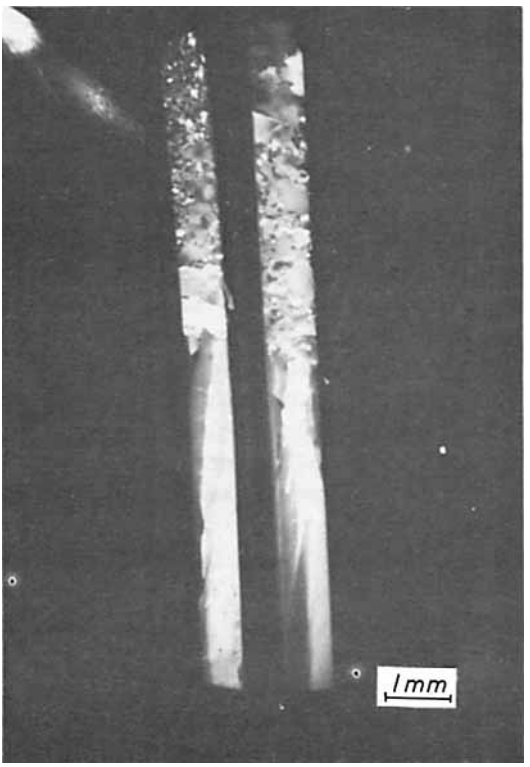

Fig. 7. Poly(oxymethylene) from solid-state polymerization of thermally oriented trioxane in a capillary.

creased the yield significantly and that the higher pulling rate gave a greater increase in yield.

As-Grown Trioxane Needles

The results described above seem to indicate that increased crystal perfection is favorable for the conversion of TOX to POM, a conclusion which is consistent with remarks in the literature.[1,19] For this reason, it came as a great surprise that trioxane needles, which are in principle quite perfect crystals, gave (under identical polymerization conditions) lower yields than bulk samples which had been melted and recrystallized to the quasi-transparent morphology. Fifteen needles transferred to sample tubes with no particular precautions to avoid bending and distortion gave yields of 8.9 ± 5.9%. (Again we note a large scatter; extremes for individual measurements were 1.65 and 22.4%.) Needles which were transferred to sample tubes with great care to avoid bending or which were polymerized directly in the receiving vessel of the purification apparatus gave yields of 23.6 ± 4.6%. This is still significantly lower than the approximately 40% observed for the melt-crystallized (quasi-transparent) crystals and much lower than the approximately 50% for samples thermally oriented at 6.6 mm/min.

There have been suggestions in the literature that monomer morphology has an influence on the degree of conversion of TOX to POM. "Aging" of TOX

crystals near T_m was found to increase yield, presumably due to increased perfection of the crystal lattice,[1] POM obtained from large crystals of TOX had higher yield, higher T_m, and better orientation than POM originating from small crystals obtained by rapid cooling of TOX.[19]

In this work, we have demonstrated a clear correlation between monomer morphology and polymer yield. We have found that yield increases in the following series: as-grown needles, TOX melt-crystallized into the quasi-transparent morphology, and thermally oriented crystals. Furthermore, we have found that by holding TOX in the molten state, one can obtain an opaque initial morphology and that conversion in this morphology is low, decreasing with increasing temperature and time in the melt.

While the increase in yield upon thermal orientation can be rationalized on the basis of a possible increase in lattice perfection, it is paradoxical that as-grown needles, which are in principle almost perfect single crystals, gave rather low yields.

The effect of time in the molten state upon the crystallization behavior of TOX can plausibly be rationalized on the basis of the effect of air dissolved in the melt. The question remains, however, why does the presence of air bubbles reduce conversion? As mentioned in the introduction, those investigators who found oxygen to affect yield observed an increase, not a decrease in yield. One possible answer is that the inclusion of air bubbles in a TOX crystal sets up strains in the lattice which impede polymerization. This argument is weakened by the fact that at postpolymerization temperatures near T_m, the molecules have considerable mobility to accommodate such strains. Another possibility is that air bubbles simply act as physical barriers and that the growing polymer fibrils stop at the bubbles, just as they stop at domain boundaries. This would not explain what appears to be a lower density of fibrils in grains containing bubbles [Fig. 8(a)] than in those that do not [Fig. 8(b)]. However, it must be noted that apparent fibril densities may be deceptive, since SEM only gives a picture of the surface, i.e., the boundaries at which the grains separated. The situation within the grains may be different. Furthermore, on occasions when beam damage was deliberately produced, the effect was to separate the fibrils, so that any possible beam damage would affect the apparent fibril density.

Repeated Polymerization Cycles

Samples of three different bulk morphologies (opaque, semitransparent, and thermally oriented) were subjected to two successive cycles of irradiation and postpolymerization. In some cases, the samples were simply reirradiated and postpolymerized a second time; in other cases, the samples were heated above the T_m of TOX (or repassed through the thermal gradient) prior to the second cycle. It appears that little additional POM was formed during the second polymerization cycle, but we make this assertion with caution due to sample inhomogeneities and loss of residual trioxane during manipulation prior to the second cycle.

For those samples which were not melted prior to the second polymerization cycle, this may mean that lattice distortion caused by formation of POM during the first cycle rendered the remainder incapable of polymerization. In fact, calorimetric work on partially polymerized TOX indicated the presence of two

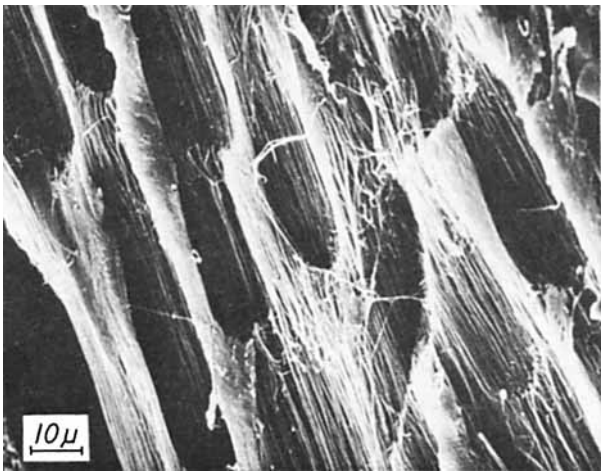

(a)

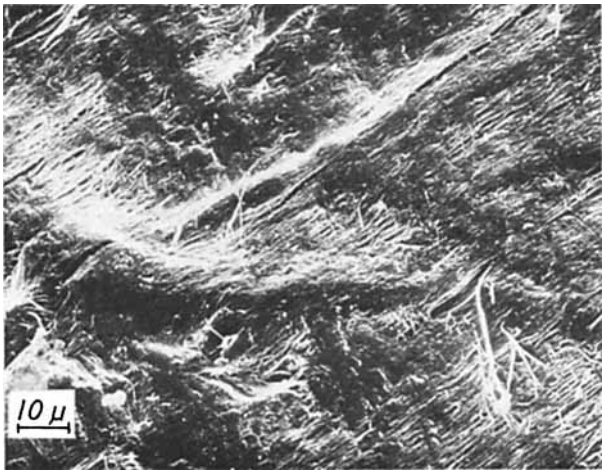

(b)

Fig. 8. Grains of poly(oxymethylene) from solid-state polymerization of bulk trioxane in opaque morphology: (a) grain containing cylindrical voids; (b) high-density grain.

forms of residual TOX—one in a separate phase and the other confined to the network of POM fibrils—demonstrating that the presence of these fibrils influences the lattice of the residual TOX.[43]

For those samples in which the residual TOX was melted prior to the second polymerization cycle, this observation may indicate either that crystallization of TOX within an environment of POM fibrils produced a morphology incapable of polymerization, or simply that residual impurities capable of impeding polymerization were concentrated into the remaining TOX during the melting.

Morphology of POM Microfibrils

Figures 9–12 show scanning electron micrographs of POM obtained from four different initial morphologies: as-grown needles, an opaque sample (with both low- and high-density grains), and a large domain from a quasi-transparent

sample. In the present series, the conversion approximately increases (of course, the conversion of individual grains from the initial opaque morphology cannot be known precisely), and we observe what appears to be a systematic variation in morphology. At the lowest conversion (Fig. 9), we have a rather low density of smooth fibrils of approximately 0.2 μ diameter. In the low-density grain, most fibrils are smooth but some exhibit nodular overgrowths (Fig. 10), while in the high-density grain, the nodulation is more pronounced (Fig. 11). Finally, in the large domain, the fibril density is still greater and very extensive nodulation is observed (Fig. 12). Although, as pointed out above, evaluation of fibril density must be done with caution, it seems clear that there is a systematic increase in nodulation, with little change in fibril diameter.

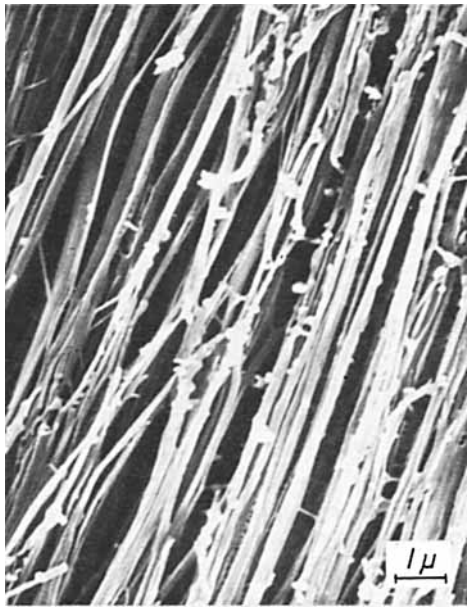

Fig. 9. Poly(oxymethylene) from solid-state polymerization of as-grown trioxane needle.

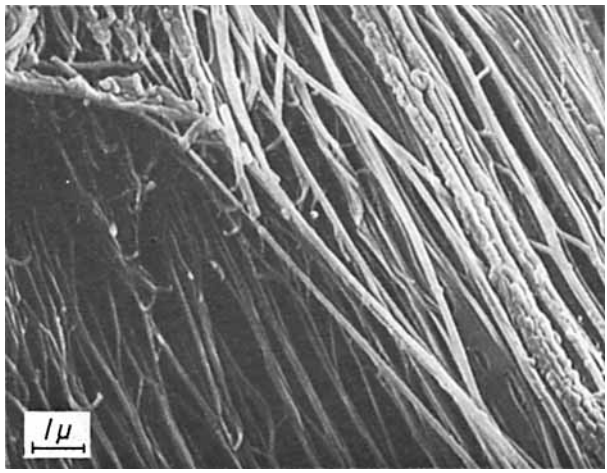

Fig. 10. Low-density grain of poly(oxymethylene) from solid-state polymerization of bulk trioxane in opaque morphology.

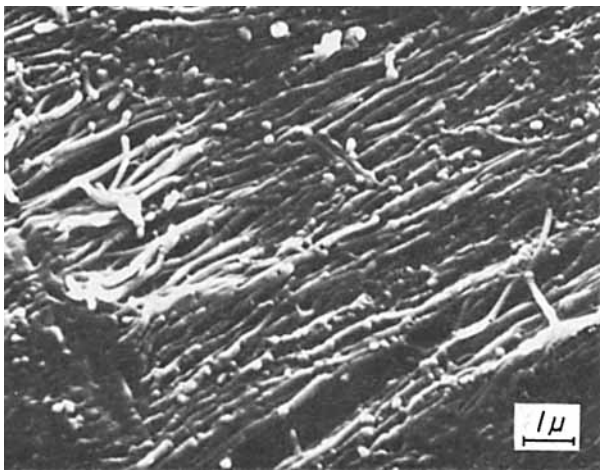

Fig. 11. High-density grain of poly(oxymethylene) from solid-state polymerization of bulk trioxane in opaque morphology.

This series of micrographs thus leads to the conclusion that an increasing "polymerizability" of the initial morphologies results in both increased density of fibrils and increased degree of nodulation (under similar irradiation and postpolymerization conditions). This conclusion lends support to Voigt-Martin's concept of multiple-stage growth in which rapid longitudinal fibril growth is followed by a slower fibril thickening.[6] Accordingly, fibril thickening would proceed via nodulation.

Figure 13 shows the grain boundary of a low-density grain in an opaque sample. It appears that the growth of the smooth fibrils reached the grain boundary, whereupon longitudinal growth stopped but polymerization continued leading noticeably to nodular fibril tips and thus to a high-density nodular surface at the grain boundary. Occasional, side-by-side fibrils have merged in common terminal nodules. These observations are again consistent with the multiple-stage growth mechanism discussed above.

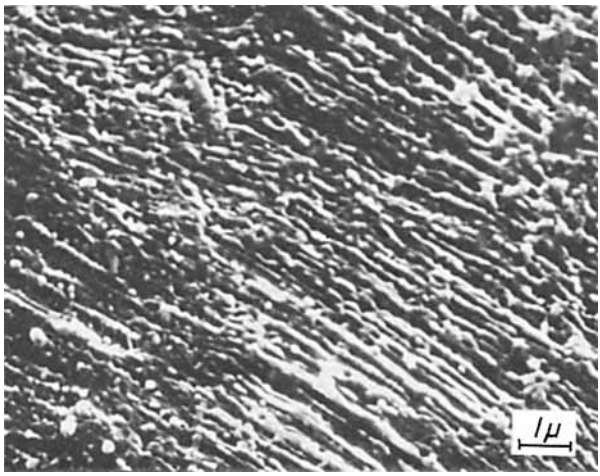

Fig. 12. Poly(oxymethylene) from solid-state polymerization of bulk trioxane in quasi-transparent morphology.

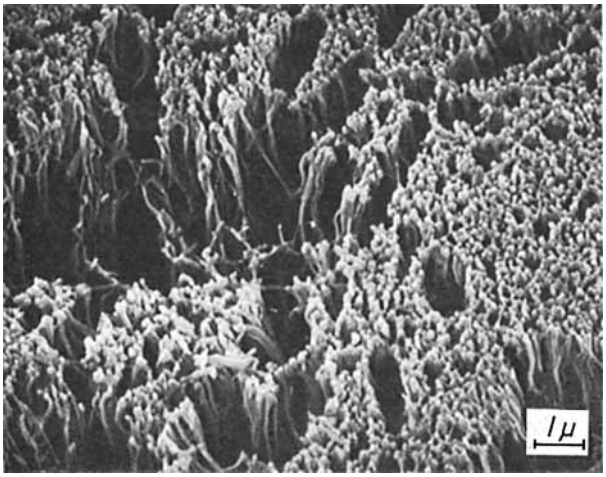

Fig. 13. Grain boundary showing tips of poly(oxymethylene) microfibrils in low-density grain from solid-state polymerization of bulk trioxane in opaque morphology.

SUMMARY AND CONCLUSIONS

Altering the initial morphology of bulk samples of trioxane by varying the temperature and/or residence time in the molten state or by thermal orientation has been shown to greatly influence yield and morphology of the resulting POM obtained after γ-irradiation and postpolymerisation. Higher polymerization yields result in both increased density of polymer fibrils and increased degree of nodulation. In addition, no further conversion of trioxane to POM could be detected in a second irradiation and postpolymerization cycle. These morphological observations are consistent with and provide further support for a multiple-stage model of polymerization, in which a rapid initial longitudinal growth giving rise to smooth fibrils is followed by fibril thickening via nodulation.

The authors wish to thank Dr. J. Marchal for helpful discussions and observations. They would also like to acknowledge Mrs. S. Zehnacker and Mr. F. Isel for valuable technical advice. Financial support for this work was provided by the Délégation Générale à la Recherche Scientifique et Technique (D.G.R.S.T N° de Décision 78.7.1030)

References

1. H. B. van der Heidje and H. Nauta, *Phil. Mag.*, **13,** 1015 (1966).
2. A. L. Hammick and A. R. Boeree, *J. Chem. Soc.*, **121,** 273 (1922).
3. H. B. van der Heidje, *Phil. Mag.*, **13,** 1055 (1966).
4. S. Okamura and K. Hayashi, *Makromol. Chem.*, **47,** 230 (1961).
5. G. Carazzolo, S. Leghissa, and M. Mammi, *Makromol. Chem.*, **60,** 171 (1963).
6. I. Voigt-Martin, *Makromol. Chem.*, **175,** 2669 (1974).
7. D. Bassett, *Nature*, **215,** 731 (1967).
8. J. P. Colson and D. H. Renecker, *J. Appl. Phys.*, **41,** 4296 (1970).
9. G. Wegner, E. W. Fischer, and A. Munoz-Escalona, *Makromol. Chem.*, **Suppl. 1,** 521 (1975).
10. S. E. Jamison and H. O. Noether, *J. Polym. Sci.*, **B1,**51 (1963).
11. S. Okamura, E. Kobayashi, and T. Higashimura, *Makromol. Chem.*, **88,** 1 (1965).

12. L. V. Babara, F. I. Dubovitskii, and A. N. Dremin, Br. Pat. 1,378,462.
13. K. Hayashi, Y. Nakase, and S. Okamura, in Proc. Meeting of the Chemical Society of Japan, Kyoto, Japan, 1962.
14. K. Hayashi, H. Ochi, and S. Ōkamura, *J. Polym. Sci.*, **A2,** 2929 (1964).
15. M. H. Rao and K. N. Rao, *Radiat. Effect*, **10,** 87 (1971).
16. H. Rao and D. S. Ballantine, *J. Polym. Sci.*, **A3,** 2579 (1965).
17. N. S. Marans and F. A. Wessels, *J. Appl. Polym. Sci.*, **9,** 3681 (1964).
18. M. L. Sagu, K. M. Sharan, J. Swarup, and K. K. Bhattacharyya, *J. Polym. Sci. Chem.*, **14,** 1815 (1976).
19. S. Okamura, K. Hayashi, and Y. Kitanishi, *J. Polym. Sci.*, **58,** 925 (1962).
20. V. Jaacks, K. Boehlke, and W. Kern, *Makromol. Chem.*, **165,** 51 (1973).
21. M. Nishii et al., *Ann. Rep. Jpn. Assoc. Radiat. Res. Polym.*, **6,** 181 (1964/1965).
22. J. P. Colson and D. H. Reneker, *J. Appl. Phys.*, **44,** 4293 (1973).
23. I. Ishigaki, A. Ito, T. Iwai, and K. Hayashi, *J. Polym. Sci., Part A-1*, **8,** 3061 (1970).
24. M. Kamachi and H. Miyana, *Nippon Kagaku Zasshi*, **85,** 815 (1964).
25. M. H. Rao and K. N. Rao, *Polym. Lett.*, **8,** 643 (1970).
26. I. Isigaki, A. Ito, T. Iwai, and K. Hayashi, *J. Polym. Sci., Part A-1*, **9,** 2511 (1971).
27. M. Saxamoto, I. Ishigaki, M. Kumakura, H. Yamashima, T. Iwai, A. Ito, and K. Hayashi, *J. Macromol. Chem.*, **1,** 639 (1966).
28. H. B. van der Heidje and P. H. G. van Kasteren, *Phil. Mag.*, **13,** 1039 (1966).
29. K. Hayashi, *Polym. Lett.*, **6,** 727 (1968).
30. I. Ishikagi, T. Iwai, and K. Hayashi, *Polym. Lett.*, **6,** 859 (1968).
31. J. Lando, N. Morossof, and B. Post, *J. Polym. Sci.*, **60,** S24 (1962).
32. S. Okamura, K. Hayashi, and M. Nishii, *J. Polym. Sci.*, **60,** S26 (1962).
33. M. L. Sagu, K. M. Swarup, D. S. Rawat, and K. K. Bhattacharyya, *Angew. Makromol. Chem.*, **62,** 45 (1977).
34. Y. Yamazawa, T. Iwai, A. Ito, and K. Hayashi, *J. Polym. Sci., Part A-1*, **9,** 257 (1971).
35. G. Adler, *J. Polym. Sci., Part A-1*, **4,** 2883 (1966).
36. G. C. Eastmond, *Polym. J.*, **4,** 392 (1973).
37. P. H. Geil, *J. Macromol. Sci.*, **A1,** 325 (1967).
38. A. Odajima, T. Ishibashi, Y. Nakase, and I. Kuriyama, *Rep. Prog. Polym. Phys. Jpn.*, **19,** 161 (1976).
39. M. Jaffe and B. Wunderlich, *Kolloid-Z. Polym.*, **216,** 203 (1967).
40. M. Takayanagi, K. Immada, A. Nagai, T. Tatsumi, and T. Matsuo, *J. Polym. Sci.*, **C16,** 867 (1967).
41. K. F. Wissbrun and A. C. Zahorchak, *J. Polym. Sci., Part A-1*, **9,** 2093 (1971).
42. J. F. Walter and P. J. Carlisle, *Chem. Eng. News*, **21,** 1250 (1943).
43. H. Nauta, *Phil. Mag.*, **13,** 1023 (1966).

Received December 10, 1980
Accepted January 21, 1981